NONLOCAL EFFECTS ON SURFACE ENHANCED RAMAN SCATTERING FROM BIMETALLIC COATED NANOPARTICLES

Y. Huang and L. Gao[*]

Department of Physics, Soochow University, Suzhou 215006, China

Abstract—We study the surface enhanced Raman scattering (SERS) from bimetallic core-shell nanoparticles by taking into account the nonlocal effect. The Gersten-Nitzan model is applied to investigate SERS from a molecule adsorbed on the nonlocal bimetallic nanoparticle. Numerical results show that there are two enhanced SERS peaks for bimetallic coated nanoparticles, and nonlocal effects will lead to less enhancement and blue-shift of SERS peaks. In addition, unusual resonant electric-field patterns are found in the nonlocal gold core in comparison with those in the local case. Our investigation is helpful for understanding some details of SERS schemes in nano-optics and plasmonics when nonlocal effects are considered.

1. INTRODUCTION

Since its first observation in 1974 [1], Surface-enhanced Raman scattering (SERS) has attracted much attention [2–4]. Now, SERS is playing an important role in surface science, spectroscopy, and detection [5] due to the high sensibility of detection with molecular identification capabilities [6, 7]. It was believed that the mechanisms for the SERS enhancement include the chemical adsorption of the metal interface [8], quantum effects [9], and the electromagnetic (EM) field enhancement at the position of the single-molecule near metal nanoparticles [10–14].

More recently, many studies aimed at the investigation of the SERS spectroscopy from different efficient substrates. For instance, SERS from silver nanosculptured thin films (STF) was investigated in detail for biosensing [15]. Gold dimer antennas with sliver layer were fabricated and SERS from such substrates were studied [16]. In

particular, with the growth of nanotechnology, a rapid development
of SERS on transition metals and other semiconductor nanostructures
were reported [17].

Of various SERS-active substrates, gold or silver nanoparticles
and their aggregates are widely used. Note that, in tiny metallic
nanostructures, the relationship between the electric displacement
field $\mathbf{D}$ and the electric field $\mathbf{E}$ is not the usual local one
$\mathbf{D}(\omega) = \varepsilon_0\varepsilon(\omega)\mathbf{E}(\omega)$ ($\varepsilon(\omega)$ is the local dielectric function), but
$\mathbf{D}(\mathbf{r}, \omega) = \varepsilon_0 \int d\mathbf{r}'\varepsilon(\mathbf{r}, \mathbf{r}', \omega)\mathbf{E}(\mathbf{r}',\omega)$, where $\varepsilon(\mathbf{r}, \mathbf{r}', \omega)$ is a spatially
dependent (nonlocal) dielectric function. For homogeneous media,
one has $\varepsilon(\mathbf{r}, \mathbf{r}', \omega) = \varepsilon(\mathbf{r} - \mathbf{r}', \omega)$, and $\mathbf{D}(\mathbf{k}, \omega) = \varepsilon_0\varepsilon(\mathbf{k}, \omega)\mathbf{E}(\mathbf{k}, \omega)$
in momentum space $\mathbf{k}$ via Fourier transformation [18]. It was
observed that taking spatial dispersion into consideration may
lead to qualitatively new phenomena such as electromagnetic wave
propagation with negative group velocity [19]. In addition, the
scattering cross section [20, 21], polarizability [22], and SERS [23] from
nonlocal metal nanoparticles were widely investigated. Later, effects of
spatial nonlocality on optical and molecular interactions with metallic
nanoshells [24], on plasmonic enhancement of Förster energy transfer
between two molecules in the vicinity of metallic nanoparticles [25],
on the optical response of a multilayered spherical system [26] were
investigated.

On the other hand, bimetallic core-shell nanoparticles are of
significance in material science because of their superior physical
properties in comparison with their individual counterparts. Besides
the application as tunable SERS substrates, bimetallic core-shell
nanoparticles, conventionally Ag-Au or Au-Ag nanoparticles, show
their advantages in immunoassay compared with monometallic
nanoshells. For bimetallic nanoparticles, near-field and far-field
scattering were studied [27], and the largest field enhancement is
found in different polarization directions for Ag-Au and Au-Ag
nanoparticles [28]. However, to our knowledge, the nonlocal responses
in bimetallic system was not addressed. Therefore, in this paper,
we would like to study the spatial nonlocality in the calculation of
SESR from a molecule adsorbed on a bimetallic core-shell nanoparticles
in the quasistatic limit. Higher-order multipolar moments should
be considered under an inhomogeneous electric field induced by the
emission of the molecule, and the Gersten-Nitzan model [11] will be
applied to study the SERS by including the nonlocal effect.

2. THEORETICAL FORMULATION

We consider surface enhanced Raman scattering from a molecule
adsorbed on a bimetallic coated nanosphere, as shown in Fig. 1.
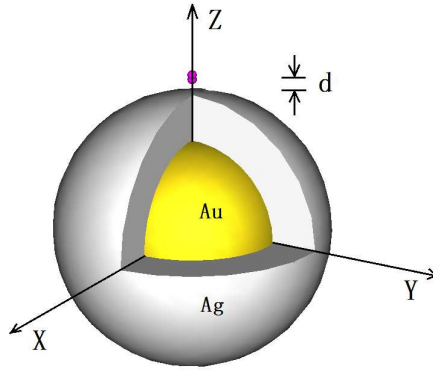
Figure 1. Schematic figure of a molecule adsorbed on a bimetallic coated nanosphere with gold core and silver shell.

Without loss of generality, the coated sphere consists of Au core of the radius a and Ag shell of the outer radius b. Both Au core and Ag shell are assumed to be nonlocal with the spatially dispersive dielectric function $\varepsilon_q(\mathbf{k}, \omega)$ ($q = c$ and s denote the core and the shell). For simplicity, the molecule adsorbed on the surface is described by an electric dipole with the dipole moment oriented normal to the nanoparticle surface at a distance d from the surface. In the quasistatic limit, the outer radius is much smaller than the incident wavelength, and we follow the works of Fuchs [22, 29] by using semiclassical infinite barrier(SCIB) model to study the nonlocal responses to the coated nanoparticle.

We write the electrostatic potentials ϕ_q ($q = c$, s, m denote the core, the shell, and the host medium) and potentials ϕ_{Dq} ($q = c$, s) with the displacement vector ($\mathbf{D} = -\nabla\phi_D$) as,

$$
\begin{cases}
\phi_c = \sum_{l=0}^{\infty} \frac{1}{\varepsilon_0} C_l a^2 F_{lc}(a, r) Y_{l0}(\theta, \phi) \\
\qquad\qquad\qquad\qquad (r < a) \\
\phi_s = \sum_{l=0}^{\infty} \frac{1}{\varepsilon_0} \left[A_l a^2 F_{ls}(a, r) + B_l b^2 F_{ls}(b, r) \right] Y_{l0}(\theta, \phi) \\
\qquad\qquad\qquad\qquad (a < r < b) \\
\phi_m = \frac{p}{4\pi\varepsilon_0} \sum_{l=0}^{\infty} -(l+1) \frac{r^l}{(b+d)^{l+2}} Y_{l0}(\theta, \phi) + \sum_{l=0}^{\infty} \frac{1}{\varepsilon_0} D_l \frac{1}{r^{l+1}} Y_{l0}(\theta, \phi) \\
\qquad\qquad\qquad\qquad (r > b),
\end{cases}
\tag{1}
$$

$$\begin{cases} \phi_{Dc} = \displaystyle\sum_{l=0}^{\infty} -C_l \frac{1}{2l+1} \frac{r^l}{a^{l-1}} Y_{l0}(\theta, \phi) & (r < a) \\[4mm] \phi_{Ds} = \displaystyle\sum_{l=0}^{\infty} -\frac{1}{2l+1} \left[A_l a^2 \frac{a^l}{r^{l+1}} + B_l b^2 \frac{r^l}{b^{l+1}} \right] Y_{l0}(\theta, \phi), & (a < r < b) \end{cases} \quad (2)$$

where A_l, B_l, C_l, D_l are the coefficients to be determined, and

$$F_{lq}(x, y) = -\frac{2}{\pi} \int_0^{\infty} \frac{j_l(kx) j_l(ky)}{\varepsilon_q(\mathbf{k}, \omega)} dk. \quad (3)$$

By applying the appropriate boundary conditions at $r = a$ and $r = b$ [22, 29],

$$\phi_c|_{r=a} = \phi_s|_{r=a}, \qquad \phi_s|_{r=b} = \phi_m|_{r=b},$$
$$\frac{\partial \phi_{Dc}}{\partial r}|_{r=a} = \frac{\partial \phi_{Ds}}{\partial r}|_{r=a}, \qquad \frac{\partial \phi_{Ds}}{\partial r}|_{r=b} = \varepsilon_0 \frac{\partial \phi_m}{\partial r}|_{r=b}, \quad (4)$$

we obtain the following matrix equation,

$$\begin{pmatrix} -a^2 F_{ls}(a,a) & -b^2 F_{ls}(b,a) & a^2 F_{lc}(a,a) & 0 \\ a^2 F_{ls}(a,b) & b^2 F_{ls}(b,b) & 0 & -b^{-l-1} \\ \frac{l+1}{2l+1} & -\frac{l}{2l+1} \cdot \frac{a^{l-1}}{b^{l-1}} & \frac{l}{2l+1} & 0 \\ \frac{l+1}{2l+1} \cdot \frac{a^{l+2}}{b^{l+2}} & -\frac{l}{2l+1} & 0 & \frac{l+1}{b^{l+2}} \end{pmatrix} \times \begin{pmatrix} A_l \\ B_l \\ C_l \\ D_l \end{pmatrix} = \begin{pmatrix} 0 \\ bQ \\ 0 \\ lQ \end{pmatrix}. \quad (5)$$

with $Q = -\frac{p}{4\pi}(l+1)\frac{b^{l-1}}{(b+d)^{l+2}}$. The l-th pole polarizability is related to the multipolar moment D_l through the relation $\alpha_l = 4\pi D_l (b + d)^{l+2}/[p(l+1)]$ [30], and one yields

$$\frac{\alpha_l}{b^{2l+1}} = \frac{-a^{l+1} b^{l+1} H_l - b^{2l+2} l(2l+1) I_l + a^l b^{l+1} J_l - b^{2l+1} l^2 K_l}{a^{2l+1} M_l - b^{2l+1} l K_l + b^{2l+2}(l+1)(2l+1) I_l + a^l b^{l+1} T_l} \quad (6)$$

with

$$H_l = l^2 (2l+1) F_{lc}(a,a) F_{ls}(a,b)$$
$$I_l = \left[-l F_{ls}(a,b)^2 + l F_{ls}(a,a) F_{ls}(b,b) + (l+1) F_{lc}(a,a) F_{ls}(b,b) \right]$$
$$J_l = l(l+1) F_{ls}(a,b)$$
$$K_l = \left[(l+1) F_{lc}(a,a) + l F_{ls}(a,a) \right]$$
$$M_l = l(l+1) F_{lc}(a,a)$$
$$T_l = l(l+1) F_{ls}(a,b)[-1 + a(2l+1) F_{lc}(a,a)].$$

If both the metallic core and shell are assumed to be local with $\varepsilon_q(\mathbf{k}, \omega) = \varepsilon_q(\omega)$, after a tedious derivation, we have

$$\frac{\alpha_l}{b^{2l+1}} = \frac{[\varepsilon_s(\omega) - \varepsilon_c(\omega)] l [l + \varepsilon_s(\omega)(l+1)](a/b)^{2l+1} + l[1 - \varepsilon_s(\omega)] S_l}{[\varepsilon_s(\omega) - \varepsilon_c(\omega)][\varepsilon_s(\omega) - 1] l(l+1)(a/b)^{2l+1} - [\varepsilon_s(\omega) l + l + 1] S_l}, \quad (7)$$

with $S_l = [\varepsilon_c(\omega)l + \varepsilon_s(\omega)(l+1)]$.

Then, we aim at the Raman cross section from a dipole-nonlocal coated sphere. Based on the Gersten-Nitzan model, the Raman cross section is expressed as [11],

$$\sigma_{\text{Raman}} = \frac{8\pi}{3}\left(\frac{\omega}{c}\right)^4 (\Delta C)^2 \left(\frac{\partial \alpha}{\partial C}\right)^2 \times \left| \frac{1}{1-\alpha G}\left[1 + \frac{2\alpha_1}{(b+d)^3}\right]\right|^4, \quad (8)$$

where ΔC is the change of nuclear coordinate, α the molecular polarizability (taken as 10Å^3), and α_1 the dipole polarizability of the coated sphere. In addition, G is the image field factor, and is written as,

$$G = \sum_l \frac{(l+1)^2}{(b+d)^{2(l+2)}}\alpha_l. \quad (9)$$

The enhancement ratio is defined as the ratio of σ_{Raman} in Eq. (8) to the one in the absence of the nanoparticle, and admits the form,

$$R = \left| \frac{1}{1-\alpha G}\left[1 + \frac{2\alpha_1}{(b+d)^3}\right]\right|^4. \quad (10)$$

3. NUMERICAL RESULTS AND DISCUSSION

To account for the spatially dispersive effects due to the nonlocal dielectric response, we adopt the simple hydrodynamic Drude model [18],

$$\varepsilon_q(\mathbf{k},\omega) = \varepsilon_{q\infty} - \frac{\omega_{qp}^2}{\omega(\omega + i\Gamma_q) - \beta^2 k^2} \quad (q = c, s), \quad (11)$$

where $\varepsilon_{q\infty}$ is the dielectric constant for $\omega \to \infty$, ω_{qp} the plasma frequency, and Γ_q the damping factor of the electrons. For a free-electron gas, we have $\beta = \sqrt{3/5}\upsilon_F$ with υ_F being the Fermi velocity. For model calculations, the plasma frequencies are $\omega_{cp} = 1.38 \times 10^{16}\,\text{s}^{-1}$ and $\omega_{sp} = 1.40 \times 10^{16}\,\text{s}^{-1}$, and Fermi velocity is $\upsilon_F = 1.39 \times 10^6\,\text{s}^{-1}$ for both Au core and Ag shell. $\varepsilon_{c\infty} = 9.84$ for Au core and $\varepsilon_{s\infty} = 3.7$ for Ag shell respectively. Moreover, to consider the interfacial scattering [31], we let the damping constant to be $\Gamma_c = \Gamma_{c,Bulk} + \upsilon_F/a$ for Au core and $\Gamma_s = \Gamma_{s,Bulk} + \upsilon_F/(b-a)$ for Ag with $\Gamma_{c,Bulk} = 10.7 \times 10^{13}\,\text{s}^{-1}$ and $\Gamma_{s,Bulk} = 3.22 \times 10^{13}\,\text{s}^{-1}$.

In Fig. 2, the SERS enhancement ratio is shown as a function of incident light wavelength λ for a molecule at $d = 1\,\text{nm}$ for a Au-Ag coated nanoparticle. It is evident that there are two plasmonic resonant modes: (1) the symmetric dipole mode at resonant long
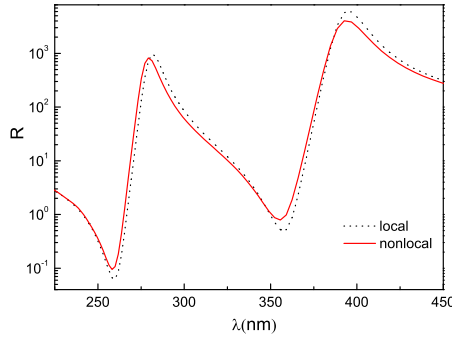
Figure 2. SERS enhancement ratio R as a function of incident wavelength λ for Au-Ag coated nanoparticles with nonlocal (solid line) and local (dotted line) dielectric functions. The relevant parameters are $a = 10\,\text{nm}$, $b = 15\,\text{nm}$, and $d = 1\,\text{nm}$.

wavelength $\lambda_{1,+}$ and (2) the antisymmetric dipole mode at resonant short wavelength $\lambda_{1,-}$, which result from two different kinds of coupling (symmetric or antisymmetric coupling) between the surface charge oscillations on two interfaces. The two resonant SERS peaks can be still observed in the experimental absorption spectra of bimetallic coated large particles [32]. In comparison with the local case, the introduction of the nonlocal term results in both the slight decrease in the magnitudes of two SERS enhanced peaks and the blue-shift of the resonant wavelengths, which are consistent with observations on SERS from a dielectric core-silver shell coated nanoparticle [33]. Actually, when the nonlocal effect is taken into account, the longitudinal modes may exist, and these modes modify the internal and external electric fields, thereby causing the shift of the resonant wavelengths. Mathematically, due to the introduction of nonlocal term, the real part of the denominator in the Drude dielectric function becomes $\omega^2 - \beta^2 k^2$ instead of ω^2 in local drude model. As a consequence, one expects the resonant frequency (wavelength) in the nonlocal case should be larger (smaller) than the one in local case, and hence takes on the blue-shift of the resonant wavelength.

Figure 3 shows a series of spectral enhancement curves for a fixed outer shell $b = 15\,\text{nm}$ and various inner radii a. Generally, the thicker the Ag shell or the smaller the Au core, the larger the magnitude of two SERS enhanced peaks is. Moreover, one observes obvious blue-shift of the resonant long-wavelength and slight red-shift of the resonant short-wavelength. Therefore, one expects one resonant peak for much smaller core at the resonant wavelength, close to pure Ag nanoparticle. To understand the two resonant modes, we extend the hybridization models [34] for air-Au nanoshell to bimetallic Au-
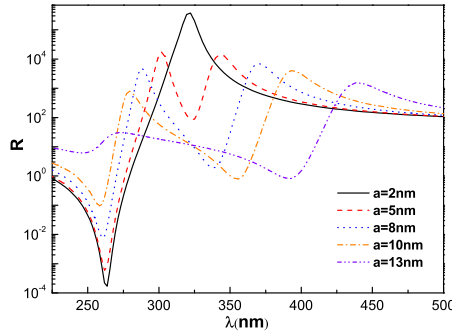
Figure 3. R as a function of λ for a Au-Ag coated nanoparticle of a fixed outer radius $b = 15\,\text{nm}$ and various a with nonlocal dielectric function.
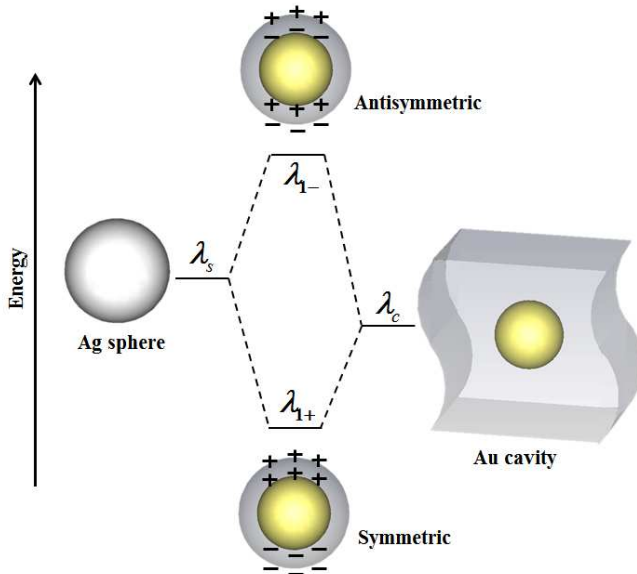
Figure 4. Schematic diagram illustrating the energy level of the plasmon hybridization in a bimetallic coated nanoparticle.

Ag coated nanoparticles (see Fig. 4). Since the resonant wavelength is slightly different from the local one, we assume that both the metallic core and metallic shell are lossless and local with the dielectric functions satisfying the Drude's model with the form, $\varepsilon_c(\mathbf{k}, \omega) = \varepsilon_{c\infty} - \omega_{cp}^2/\omega^2$ and $\varepsilon_s(\mathbf{k}, \omega) = \varepsilon_{s\infty} - \omega_{sp}^2/\omega^2$. The corresponding two plasmonic modes in the SERS enhancement for Au-Ag coated nanospheres mainly come from the interacting dipole plasmons of solid

Ag sphere (sphere-like mode) and the dipole plasmons of Au cavity sphere (cavity-like mode). In our situation, the void (or cavity)-like and sphere-like resonance wavelengths for Au-Ag coated nanospheres can be derived analytically. That is, the sphere-like modes can be excited from the system in which the Ag nanoparticles are suspended in the air host medium. Hence, the resonant wavelength is derived to be $\lambda_s = 2\pi c\sqrt{\varepsilon_{s\infty}+2}/\omega_{sp}$. Similarly, the cavity-like modes can be excited from the system in which Au nanoparticles are embedded in the Ag host medium and resonant short-wavelength is obtained such as $\lambda_c = 2\pi c\sqrt{(\varepsilon_{c\infty}+2\varepsilon_{s\infty})/(\omega_{cp}^2+2\omega_{sp}^2)}$. As $\lambda_s < \lambda_c$, the antisymmetric coupling between solid sphere and spherical cavity gives rise to higher energy (or short wavelength) mode at $\lambda_{1,-}$, which is mainly dependent on the plasmon of outer surface (Ag spherical mode). On the other hand, the symmetric coupling, which gives rise to lower energy mode (or long wavelength) $\lambda_{1,+}$, which is mainly dependent on the plasmon of inner surface (Au cavity mode in which the cavity is full of Au). The interaction between the sphere and cavity plasmonic modes can be tuned by changing the thickness of the shell. Note that due to the fact that $\lambda_c < \lambda_s$ for air-Ag nanoshells, the antisymmetric (symmetric) mode is mainly dependent on Ag-cavity (Ag-sphere) mode, which is slightly different from the case for Au-Ag coated nanoparticles (see Fig. 4).

By letting the denominators of Eqs. (6) or (7) be zero [35], we obtain the dipole resonant wavelengths for $l = 1$ analytically,

$$\lambda_{1,\pm}^2 = 4\pi^2 c^2 \frac{2f}{-g \mp \sqrt{g^2-4fh}}, \tag{12}$$

with

$$
\begin{aligned}
f &= (\varepsilon_{c\infty}+2\varepsilon_{s\infty})(\varepsilon_{s\infty}+2) + 2(\varepsilon_{c\infty}-\varepsilon_{s\infty})(\varepsilon_{s\infty}-1)(a/b)^3, \\
g &= -(\varepsilon_{s\infty}+2)\omega_{cp}^2 - (\varepsilon_{c\infty}+4\varepsilon_{s\infty}+4)\omega_{sp}^2 \\
&\quad -2\Big[(\varepsilon_{s\infty}-1)\omega_{cp}^2 + (\varepsilon_{c\infty}-2\varepsilon_{s\infty}+1)\omega_{sp}^2\Big](a/b)^3, \\
h &= \omega_{cp}^2\omega_{sp}^2 + 2\omega_{sp}^2\Big[\omega_{sp}^2 + \big(\omega_{cp}^2-\omega_{sp}^2\big)(a/b)^3\Big].
\end{aligned}
$$

Equation (12) are the general analytic expressions for the dipole plasmon resonant short and long wavelengths for the bimetallic nanospheres. For an Ag spherical nanoparticle, $a = 0$, and for a Ag cavity full of Au, $b = \infty$, Eq. (12), respectively, reduces to $\lambda_{1,+} = \lambda_c$ and $\lambda_{1,-} = \lambda_s$.

The dependences of two resonant wavelengths for SERS enhancement peaks on the ratio $(a/b)^3$ are shown in Fig. 5. The nonlocal results shown in Fig. 5 are obtained via numerical methods
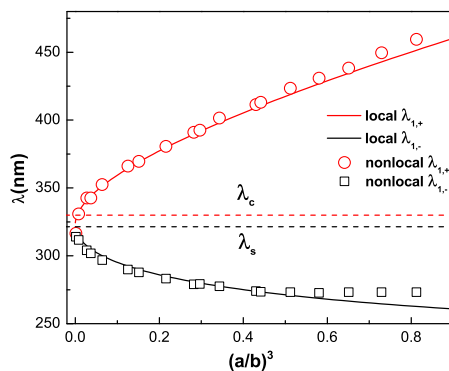
Figure 5. Two resonant wavelengths for SERS enhancment peaks as a function of the ratio $(a/b)^3$. Resonant wavelengths for symmetric and antisymmetric modes, determined by Eq. (12), are represented by red and black solid lines respectively. Nonlocal cases are shown with hollow circles and squares.

since it is rather difficult to get an analytical solution from Eq. (6). It is evident that with decreasing of the ratio $(a/b)^3$, the resonant long-wavelength is decreased obviously, while the resonant short-wavelength is increased slightly, which in accordance with our analytical results based on Eq. (12). Actually, the surface resonant wavelength is related to the intrinsic wavelength of oscillatory electrons in nanoparticles. If the oscillatory electrons are strongly bounded, the surface resonant energy should be large and the resonant wavelength is short. On the contrary, the resonant wavelength should be long when the electrons are weakly bounded. With the decrease of the core radius, the proportion of the Au^{3+} becomes small and the attractive force between Au ion and the electrons in Ag shell becomes weak, leading to the increase of the bound grade and the blue-shift of the resonant wavelength of $\lambda_{1,+}$ obviously. However, at the outer interface, with the decrease of Au core, due to the weak attractive force between Au ion and the electrons in Ag shell, the electrons can be easily cross the outer interface, resulting in the red-shift of the resonant wavelength $\lambda_{1,-}$.

Next, we would like to investigate the near-field distributions at two surface resonant wavelengths with both local and nonlocal theories. It is known that the existence of the molecule (or a dipole) will amplify the field around itself significantly. As a consequence, it is difficult for us to recognize clearly the field distributions of the other regions away from the molecule. To illustrate them more clearly, we move the molecule a little farther away from the outer surface of the coated nanoparticle. For both local and nonlocal cases, we

find that at resonant long wavelength, the fields in the core and in the air medium close to the interface between the shell and the medium are largely enhanced, while the fields in the shell are enhanced at resonant short wavelength, which demonstrates our discussions in previous paragraphs. To one's interest, when the nonlocality is taken into account, the electric field in gold core is oscillating (see Figs. 6(c) and (d)), which is quite different from the local one (see Figs. 6(a)and (b)). The resonant field patterns clearly demonstrate that the longitudinal bulk plasmon modes may exist in the nonlocal particles especially in Au core [18, 21]. To show such oscillating modes clearly, we give the near-field distributions in the same structure at low frequency with nonlocal theory but the distance $d = 500$ nm, as shown in Fig. 7. Note that the resonant electric field in gold core is not as symmetric as the one in pure gold spheres [18] due to the applied dipole fields instead of the incident plane waves.
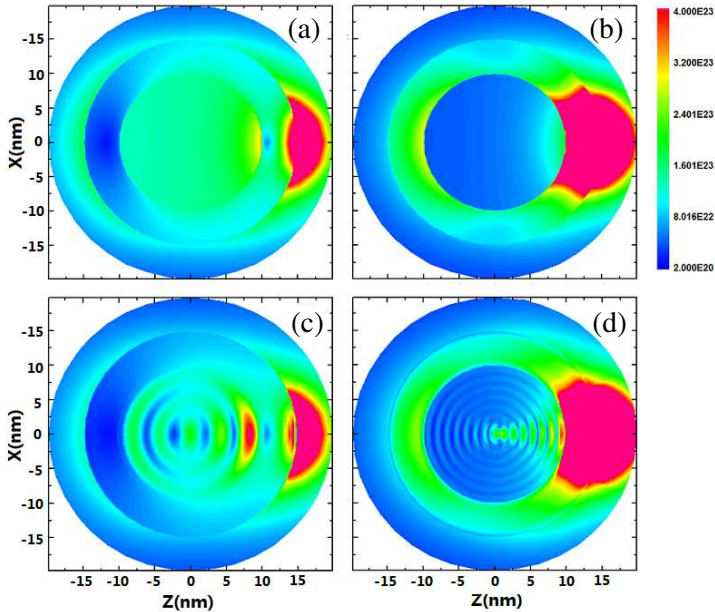
Figure 6. Near-field distributions for Au-Ag coated nanoparticle at the long wavelength $\lambda_{1,+} = 396$ nm for (a) and (c), short wavelength $\lambda_{1,-} = 280$ nm for (b) and (d). Both (top) local and (bottom) nonlocal calculations are shown. Other parameters are $a = 10$ nm, $b = 15$ nm, and $d = 5$ nm.
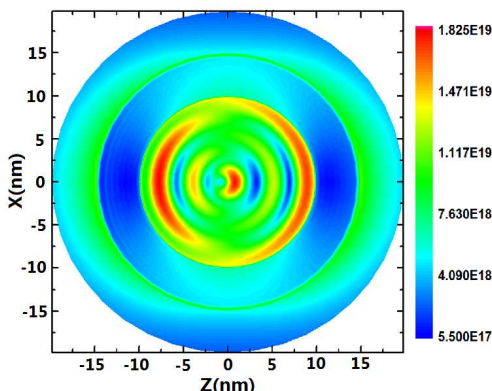
Figure 7. Near-field distributions for Au-Ag coated nanoparticle at resonant long wavelength with nonlocal theory. Parameters are $a = 10\,\mathrm{nm}$, $b = 15\,\mathrm{nm}$, and $d = 500\,\mathrm{nm}$.

4. CONCLUSION

In this work, we have investigated the SERS enhancement spectra from Au-Ag bimetallic coated nanoparticles with nonlocal theory in the quasistatic limit. We derive the multipole polarizability from the coated nanoparticles based on the works of Fuchs et al. [22], and present the formula for the SERS enhancement ratio with the aid of the Gersten-Nitzn model. Numerical results show that the SERS enhancement ratios at two resonant wavelengths are slightly decreased, and two resonant wavelengths are slightly blue-shifted when the nonlocality is included. Moreover, when the spatial nonlocality is taken into account, the near-field distributions in the gold core region are found to be oscillating due to the existence of longitudinal bulk plasmon modes.

Some comments are in order. First, the multipolar polarizability is derived in the quasistatic limit. To keep the quasistatic approximation to be valid such as $k_q b \leq 0.1$ [k_q ($q = c, s$) is the wave number in the core or the shell], according to our qualitative analysis, the size of coated particles b is less than $20\,\mathrm{nm}$ in the studied wavelength range. On the other hand, when the nanoparticles are larger, the effect of radiation damping and destructive interferences should be considered. To incorporate such electrodynamic corrections, α_l is replaced by [36]

$$\alpha_l^{eff} = \left[1 - \mathrm{i} \frac{(l+1)k_0^{2l+1}}{l(2l-1)!!(2l+1)!!} \alpha_l \right]^{-1} \alpha_l. \qquad (13)$$

Second, it was reported that the hot spots could also give rise to increased SERS signal, because they facilitate enhanced optical fields, which in turn contribute to the electromagnetic enhancement when a molecule is in the vicinity of these spots. The hot spots in bimetallic coated nanoparticles with pinholes were investigated by means of experimental method [37]. On the theoretical side, the nonlocality should be involved to study the hot spots in the enhancement of Raman signal due to the pinholes or other nano-defects at rather small scale. In the end, to compute absolute Raman, fluorescence, absorption cross sections and spectra for arbitrary irradiation levels, one should involve a quantum optical description of a model molecule [13], of which molecular dynamics is calculated using a density matrix approach. By using this method, we shall give detailed information about the enhancement and quenching of single-molecule fluorescence [38] by taking into account the nonlocality or spatial dispersion.

ACKNOWLEDGMENT

REFERENCES

1. Fleischmann, M., P. J. Hendra, and A. Mcquilla, "Raman spectra of pyridine adsorbed at a silver electrode," *Chem. Phys. Lett.*, Vol. 26, 163–166, 1974.
2. Tian, Z. Q. and B. Ren, "Adsorption and reaction at electrochemical interfaces as probed by surface-enhanced Raman spectroscopy," *Annu. Rev. Phys. Chem.*, Vol. 55, 197–229, 2004.
3. Wustholz, K. L., C. L. Brosseau, F. Casadio, and R. P. van Duyne, "Surface-enhanced Raman spectroscopy of dyes: From single molecules to the artists canvas," *Physical Chemistry Chemical Physics*, Vol. 11, 7350–7359, 2009.
4. Stiles, P. L., F. A. Dieringer, N. C. Shah, and R. P. van

Duyne, "Surface-enhanced Raman spectroscopy," *Annu. Rev. Anal. Chem.*, Vol. 1, 601–626, 2008.

5. Cao, Y. C., R. Jin, and C. A. Mirkin, "Nanoparticles with Raman spectroscopic fingerprints for DNA and RNA detection," *Science*, Vol. 297, 1536–1540, 2002.

6. Nie, S. and S. R. Emory, "Probing single molecules and single nanoparticles by surface-enhanced Raman scattering," *Science*, Vol. 275, 1102–1106, 1997.

7. Kneipp, K., Y. Wang, H. Kneipp, T. Perelman, I. Itzkan, R. R. Dasari, and M. S. Feld, "Single molecule detection using surface-enhanced Raman scattering (SERS)," *Phys. Rev. Lett.*, Vol. 78, 1667–1670, 1997.

8. Emel'yanov, V. and T. V. Koroteev, "Giant Raman scattering of light by molecules adsorbed on the surface of a metal," *Sov. Phys. Usp.*, Vol. 24, 864–873, 1981.

9. Pustovit, V. N. and T. V. Shahbazyan, "Microscopic theory of surface-enhanced Raman scattering in noble-metal nanoparticles," *Phys. Rev. B*, Vol. 73, 085408, 2006.

10. Kerker, M., D. S. Wang, and H. Chew, "Surface enhanced Raman scattering (SERS) by molecules adsorbed at spherical particles: Errata," *Appl. Opt.*, Vol. 19, 4159–4174, 1980.

11. Gersten, J. and A. Nitzan, "Electromagnetic theory of enhanced Raman scattering by molecules adsorbed on rough surfaces," *J. Chem. Phys.*, Vol. 73, 3023–3037, 1980.

12. Schatz, G. C. and R. P. van Duyne, "Electromagnetic mechanism of surface-enhanced spectroscopy," *Handbook of Vibrational Spectroscopy*, John Wiley and Sons, Ltd., 2006.

13. Xu, H. X., X. H. Wang, M. P. Persson, and H. Q. Xu, "Unified treatment of fluorescence and Raman scattering processes near metal surfaces," *Phys. Rev. Lett.*, Vol. 93, 243002, 2004.

14. Yin, Y. D., L. Gao, and C. W. Qiu, "Electromagnetic theory of tunable SERS manipulated with spherical anisotropy in coated nanoparticles," *J. Phys. Chem. C*, Vol. 115, 8893–8899, 2011.

15. Shalabney, A., C. Khare, J. Bauer, B. Rauschenbach, and I. Abdulhalim, "Detailed study of surface-enhanced Raman scattering from metallic nanosculptured thin films and their potential for biosensing," *J. Nanophoton.*, Vol. 6, No. 1, 061605, 2012.

16. Höflich, K., "Plasmonic dimer antennas for surface enhanced Raman scattering," *Nanotechnology*, Vol. 23, 185303, 2012.

17. Wang, X. T. and W. S. Shi, "Surface-enhanced Raman scattering

(SERS) on transition metal and semiconductor nanostructures," *Physical Chemistry Chemical Physics*, Vol. 14, 5891–5901, 2012.

18. McMahon, J. M., S. K. Gray, and G. C. Schatz, "Nonlocal optical response of metal nanostructures with arbitrary shape," *Phys. Rev. Lett.*, Vol. 103, 097403, 2009.

19. Mikki, S. M. and A. A. Kishk, "Electromagnetic wave propagation in non-local media — Negative group velocity and beyond," *Progress In Electromagnetics Research B*, Vol. 14, 149–174, 2009.

20. Ruppin, R., "Optical properties of a plasma sphere," *Phys. Rev. Lett.*, Vol. 31, 1434–1437, 1973.

21. Raza, S., M. Wubs, and N. A. Mortensen, "Unusual resonances in nanoplasmonic structures due to nonlocal response," *Phys. Rev. B*, Vol. 84, 121412, 2011.

22. Dasgupta, B. B. and R. Fuchs, "Polarizability of a small sphere including nonlocal effects," *Phys. Rev. B*, Vol. 24, 554–561, 1981.

23. Leung, P. T. and W. S. Tse, "Nonlocal electrodynamic effect on the enhancement factor for surface enhanced Raman scattering," *Solid State Commun.*, Vol. 95, 39–44, 1995.

24. Chang, R. and P. T. Leung, "Nonlocal effects on optical and molecular interactions with metallic nanoshells," *Phys. Rev. B*, Vol. 73, 125438, 2006.

25. Xie, H. Y., H. Y. Chung, P. T. Leung, and D. P. Tsai, "Plasmonic enhancement of Förster energy transfer between two molecules in the vicinity of a metallic nanoparticle: Nonlocal optical effects," *Phys. Rev. B*, Vol. 80, 155448, 2009.

26. Chung, H. Y., G. Y. Guo, H. P. Chiang, D. P. Tsai, and P. T. Leung, "Accurate description of the optical response of a multilayered spherical system in the long wavelength approximation," *Phys. Rev. B*, Vol. 82, 165440, 2010.

27. Bruzzone, S., M. Malvaldi, G. P. Arrighini, and C. Guidotti, "Near-field and far-field scattering by bimetallic nanoshell systems," *J. Phys. Chem. B*, Vol. 110, 11050–11054, 2006.

28. Wu, D. J., X. D. Xu, and X. J. Liu, "Electric field enhancement in bimetallic gold and silver nanoshells," *Solid State Commun.*, Vol. 148, 163–167, 2008.

29. Rojas, R., F. Claro, and R. Fuchs, "Nonlocal response of a small coated sphere," *Phys. Rev. B*, Vol. 37, 6799–6807, 1988.

30. Fan, C. Z., J. P. Huang, and K. W. Yu, "Dielectrophoresis of an inhomogeneous colloidal particle under an inhomogeneous field: A first-principles approach," *J. Phys. Chem. B*, Vol. 110, 25665-25670, 2006.

31. Westcott, S. L., J. B. Jackson, C. Radloff, and N. J. Halas, "Relative contributions to the plasmon line shape of metal nanoshells," *Phys. Rev. B*, Vol. 66, 155431, 2002.

32. Steinbruck, A., A. Csaki, G. Festag, and W. Fritzsche, "Preparation and optical characterization of core-shell bimetal nanoparticles," *Plasmonics*, Vol. 1, 79, 2006.

33. Goude, Z. E. and P. T. Leung, "Surface enhanced Raman scattering from metallic nanoshells with nonlocal dielectric response," *Solid State Commun.*, Vol. 143, 416–420, 2007.

34. Prodan, E., C. Radloff, N. J. Halas, and P. Nordlander, "A hybridization model for the plasmon response of complex nanostructures," *Science*, Vol. 302, 419–422, 2003.

35. Li, B. Q. and C. H. Liu, "Long-wave approximation for hybridization modeling of local surface plasmonic resonance in nanoshells," *Opt. Lett.*, Vol. 36, 247–249, 2011.

36. Colas des Francs, G., "Molecule non-radiative coupling to a metallic nanosphere: An optical theorem treatment," *Int. J. Mol. Sci.*, Vol. 10, 3931–3936, 2009.

37. Pavan Kumar, G. V., S. Shruthi, B. Vibha, B. A. Ashok Prddy, T. K. Kundu, and C. Narayana, "Hot spots in Ag core-Au shell nanoparticles potent for surface-enhanced Raman scattering studies of biomolecules," *J. Phys. Chem. C*, Vol. 111, 4388–4392, 2007.

38. Anger, P., P. Bharadwaj, and L. Novotny, "Enhancement and quenching of single-molecule fluorescence," *Phys. Rev. Lett.*, Vol. 96, 113002, 2006.